

Backbone modification of a polypeptide drug alters duration of action *in vivo*

Ross W Cheloha¹, Akira Maeda², Thomas Dean²,
Thomas J Gardella² & Samuel H Gellman¹

Systematic modification of the backbone of bioactive polypeptides through β -amino acid residue incorporation could provide a strategy for generating molecules with improved drug properties, but such alterations can result in lower receptor affinity and potency. Using an agonist of parathyroid hormone receptor-1 (PTHr1), a G protein-coupled receptor in the B-family, we present an approach for $\alpha \rightarrow \beta$ residue replacement that enables both high activity and improved pharmacokinetic properties *in vivo*.

B-family G protein-coupled receptors are activated by polypeptide hormones containing >25 residues. Several widely used drugs, all long peptides, act on receptors in this class; efforts to activate these receptors with small molecules have been largely unsuccessful. However, polypeptide drugs frequently suffer from poor stability *in vivo* because of protease-catalyzed degradation. We used PTHR1 signaling to evaluate a strategy for creating active and biostable backbone-modified analogs of the well-known agonist PTH(1-34). PTH is an 84-residue protein that controls key physiological processes, including the maintenance of extracellular levels of calcium and phosphate and bone homeostasis¹. PTH(1-34) matches full-length PTH in potency and efficacy at PTHR1 and is the active ingredient in the osteoporosis drug teriparatide (Forteo). As with many other peptide-based therapeutics, PTH(1-34) has a short half-life in the bloodstream (<30 min)². Therapeutic effects for osteoporosis treatment appear to be maximized by pulsatile rather than continuous exposure to PTH(1-34), but the optimal exposure cycle is unclear³. We generated new analogs of PTH(1-34) by replacing selected α -amino acid residues with homologous β -amino acid residues, an unconventional approach that alters the backbone but can maintain the natural side chain complement. The results show that this technically straightforward strategy can provide hormone analogs that display native-like receptor activation potencies and prolonged residency in the bloodstream.

The C-terminal portion of PTH(1-34) forms an α -helix upon binding to the receptor, but the bioactive conformation of the N-terminal segment is unknown. The backbone-modification strategy described here is based on previous studies showing that α -helical segments

involved in protein-recognition processes can be mimicked by oligomers containing mixtures of α and β residues^{4,5}. Other types of unnatural oligomers, such as peptides composed of D- α -amino acid residues⁶, peptoids⁷ and β -peptides⁸, have been explored for functional mimicry of bioactive α -helices; however, none of these alternative molecular scaffolds allows faithful mimicry of a long α -helix⁵, as required for potent analogs of PTH. In previous studies, PTH analogs containing one to three β -residue replacements were used to probe local conformational requirements, and many of these replacements caused profound declines in agonist activity^{9,10}. The peptide hormone GLP-1(7-37), which activates a different B-family G protein-coupled receptor, parallels PTH(1-34) in that the C-terminal portion is α -helical when bound to the receptor¹¹; recent efforts to replace the α -helix with a purely β -residue segment essentially abolished activity¹². In contrast, we show that proper choice of β -residue identity and location allows $\alpha \rightarrow \beta$ residue replacement at up to seven distributed sites with maintenance of PTH(1-34)-like potency, but alteration of the pharmacokinetic profile.

We prepared all four PTH(1-34) analogs containing five $\alpha \rightarrow \beta^3$ replacements in an $\alpha\alpha\alpha\beta$ pattern¹³ within the C-terminal region (A5-D5 in Fig. 1a). Native α -residues were replaced with β^3 homologs (Fig. 1b), except for His-32, which was conservatively replaced with β^3 -homoglutamine. Thus, natural side chains were retained in the resulting α/β -peptides, but the backbone contained additional CH₂ units. Introduction of $\alpha \rightarrow \beta^3$ substitutions using this design strategy has been shown to yield α/β -peptides that mimic α -helical segments of proteins¹³, and we therefore expected that PTH(1-34) analogs A5-D5 would be competent to mimic the helical conformation observed in the crystal structure of PTH(15-34) bound to the extracellular domain of human PTHR1 (ref. 14). Alternative strategies for introducing $\alpha \rightarrow \beta$ replacements in peptide hormones have been largely unsuccessful in terms of retaining native potency^{9,10,12}. α/β -peptides A5-D5 were easily prepared by conventional solid-phase synthesis.

PTHr1 has two distinct functional states: RG, which forms when the intracellular portion contacts G_{αS} (a heterotrimeric G-protein responsible for activating adenylate cyclase upon receptor activation); and R⁰, which forms independent of G_{αS}^{15,16}. An agonist's affinity for the RG state correlates with PTHR1 activation potency, whereas R⁰ affinity correlates with the duration of some *in vivo* responses^{16,17}. We used well-established radioligand-displacement assays^{15,16} to show that the $\alpha \rightarrow \beta^3$ replacements influence receptor binding, and the effect of each $\alpha\alpha\alpha\beta$ pattern varies between R⁰ and RG. In contrast to α/β -peptides A5-C5, D5 mimics the binding profile of PTH(1-34), perhaps because the $\alpha \rightarrow \beta^3$ replacement sites in D5 are mostly oriented away from the receptor surface (Fig. 1c)¹³. Extensions of this $\alpha\alpha\alpha\beta$ pattern produced D6 and D7, which retained high affinity for the R⁰ and RG states of PTHR1 (Table 1 and Supplementary Table 1).

¹Department of Chemistry, University of Wisconsin, Madison, Wisconsin, USA. ²Endocrine Unit, Massachusetts General Hospital and Harvard Medical School, Boston, Massachusetts, USA. Correspondence should be addressed to T.J.G. (gardella@helix.mgh.harvard.edu) or S.H.G. (gellman@chem.wisc.edu).

Received 13 December 2013; accepted 5 May 2014; published online 15 June 2014; doi:10.1038/nbt.2920

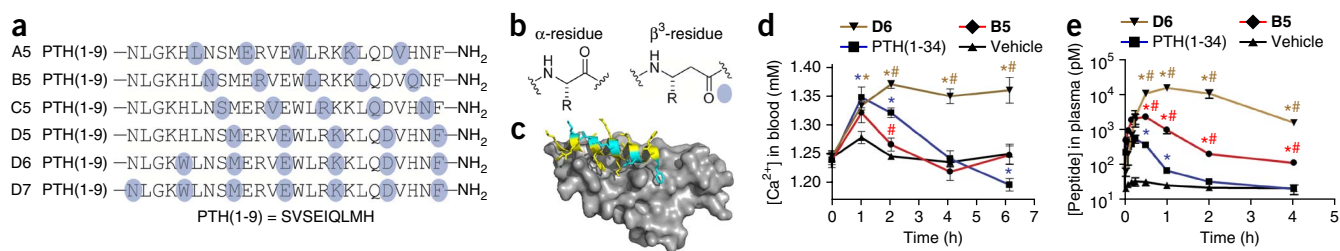


Figure 1 Backbone-modified analogs of PTH(1-34) are active *in vivo* and display improved pharmacokinetic properties. **(a)** The α/β -peptide analogs of PTH(1-34) used in this study. The conventional single-letter code is used to indicate proteogenic α -amino acid residues. Blue dots indicate sites of $\alpha \rightarrow \beta^3$ replacement; each β^3 residue bears the side chain of the α residue indicated by the letter. **(b)** Structures of a generic α -amino acid residue and the homologous β^3 -amino acid residue. **(c)** Positions of $\alpha \rightarrow \beta^3$ modification sites in α/β -peptide **D5** mapped onto the crystal structure of PTH(15-34) bound to the extracellular domain of PTHR1 (PDB 3C4M; ref. 14). The extracellular domain is shown as a gray surface, and the peptide ligand is shown in yellow, with sites of $\alpha \rightarrow \beta^3$ modification shown in blue. Extracellular domain residues not interacting with PTH (residues 155-175) have been hidden to enable visualization of the PTH-PTHR1 interaction. **(d)** Effects of PTH(1-34), **B5** and **D6** on blood Ca^{2+} levels (mean \pm s.e.m.) in mice ($n = 5$) at a dose of 20 nmol/kg. * $P < 0.05$ versus vehicle, # $P < 0.05$ versus PTH(1-34). **(e)** Concentrations of PTH(1-34), **B5** or **D6** in plasma (mean \pm s.e.m.) from blood withdrawn from mice ($n = 3$) at times indicated following subcutaneous injection at the dose described above. Compound concentrations were determined by submitting mouse plasma to a cAMP GloSensor assay (see **Supplementary Fig. 5** for details). * $P < 0.05$ versus vehicle, # $P < 0.05$ versus PTH(1-34) using negative log[compound] concentrations. Significance measurements for first four time points are reported in **Supplementary Figure 5**. Source data provided in **Figure 1** source data file.

Agonist activities were determined by monitoring cAMP production in HEK293 cells that stably express human (h)PTHR1 and the GloSensor cAMP reporter¹⁸. All six α/β -peptides proved to be full agonists (**Table 1** and **Supplementary Table 2**). Most were comparable to PTH(1-34) in terms of potency, as indicated by EC_{50} values for cAMP production.

For *in vivo* studies, we selected analogs **B5** and **D6** for comparison with PTH(1-34). **D6** was chosen because this analog is indistinguishable from PTH(1-34) in terms of PTHR1 RG and R^0 affinities and agonist potency (**Table 1**). **B5** was chosen because the receptor-binding profile differs substantially from that of PTH(1-34): this analog matches PTH(1-34) in potency and RG affinity but has ~17-fold lower affinity for R^0 . Both analogs contain a substantial complement of $\alpha \rightarrow \beta^3$ replacements, which was predicted to provide protection against proteolysis in the C-terminal region. Because the *in vivo* assessment involved mice, we complemented the *in vitro* studies involving hPTHR1 (**Table 1**) with analogous measurements based on rat (r)PTHR1. The rat and mouse receptors have 98% sequence identity, whereas the human and mouse receptors have only 90% sequence identity. Trends identified for receptor affinities and agonist activities with hPTHR1 were generally mirrored with rPTHR1 (**Supplementary Tables 3** and **4**).

Subcutaneous injection of PTH(1-34), **D6** or **B5** led to different calcemic responses in mice (**Fig. 1d**). PTH(1-34) causes the blood concentration of Ca^{2+} to rise transiently¹⁶. In comparison, the Ca^{2+}

concentration rise caused by **D6** was longer, and that caused by **B5** was shorter. **D6** persisted considerably longer *in vivo* than did PTH(1-34) (**Fig. 1e**), which presumably underlies the prolonged signaling of this analog. We propose that this prolonged bloodstream residence stems from resistance to proteolysis conferred by the large number and broad distribution of β residues in **D6**. Comparison of trypsin digestion of **D6** and PTH(1-34) showed that the β residues protect nearby amide bonds (**Supplementary Note 1** and **Supplementary Fig. 1**). The calcemic effect durations for PTHR1 agonists are correlated with affinities for the R^0 state^{16,17}. The increased calcemic effect duration of PTH(1-34) relative to **B5** is consistent with this correlation because PTH(1-34) has a substantially higher R^0 affinity than does **B5** (**Supplementary Tables 1** and **3**). It is noteworthy that the relative R^0 affinities of PTH(1-34) and **B5** appear to be more important than relative pharmacokinetic properties of these two molecules (**Fig. 1e**) in terms of calcemic effect duration.

We have shown that potent analogs of the medically important peptide PTH(1-34) can be generated by replacing a subset of native α -amino acid residues with homologous β^3 residues. Our observations raise the possibility that α/β analogs of other partially α -helical peptide hormones, including other B-family G protein-coupled receptor ligands, may prove to be a good source of pharmacokinetically improved agonists for receptors that mediate important physiological processes but are not amenable to activation by small molecules. The backbone modification approach may ultimately provide compounds of biomedical utility; for example, the improved *in vivo* lifetime and enhanced signal duration of **D6** relative to PTH(1-34) could allow less frequent dosing for forms of hypoparathyroidism that benefit from twice-daily PTH(1-34) injections^{16,19}. The potential of PTH analogs that induce prolonged PTHR1 signaling for osteoporosis therapy is unclear at present. Such agents might induce bone resorption rather than bone formation, as seen in animals that receive continuous rather than pulsatile PTH(1-34) treatment³; however, a PTH(1-34)-human IgG Fc fusion protein that displays prolonged *in vivo* half-life relative to PTH(1-34) is a potent stimulator of bone growth²⁰. The high hPTHR1 activation potency, improved pharmacokinetics and weak *in vivo* Ca^{2+} mobilization activity demonstrated by **B5** represent favorable characteristics in this regard, but the bone anabolic properties of this α/β -peptide remain to be characterized. Because peptide hormone analogs containing $\alpha \rightarrow \beta^3$ replacements can be readily prepared by conventional solid-phase synthesis using commercially available building blocks, further exploration

Table 1 Binding and signaling properties of PTH analogs for hPTHR1^a

	Binding (hPTHR1) ^{b-d}		cAMP (hPTHR1) ^e	
	R^0 IC_{50} (nM)	RG IC_{50} (nM)	EC_{50} (nM)	Max^f
PTH(1-34)	1.1	0.10	0.17	1.00
A5	310	2.71	1.66	1.12
B5	19	0.086	0.11	0.98
C5	11	0.40	0.20	1.01
D5	1.7	0.28	0.26	1.03
D6	2.0	0.065	0.13	0.87
D7	3.5	0.24	0.39	0.85

^aValues are means of $n \geq 4$ experiments, each performed in duplicate. See **Supplementary Tables 1** and **3** for uncertainties associated with each parameter and sample sizes used for individual analogs. See methods section on data calculations for discussion of data fitting and statistics. ^bAssays were performed in membranes prepared from COS-7 cells transiently transfected to express WT hPTHR1. ^c R^0 assays used ¹²⁵I-PTH(1-34) tracer and contained GTP γ S (1×10^{-5} M). ^dRG assays used ¹²⁵I-M-PTH(1-15) tracer and membranes from cells co-transfected to express a high affinity $\text{G}_{\alpha s}$ mutant. ^eAssays were performed in GP-2.3 cells expressing hPTHR1-WT and the luciferase-based, GloSensor cAMP reporter. ^fValues are luminescence counts per second relative to PTH(1-34) observed 12–16 min after ligand addition.

of PTH analogs and extension of this approach to other peptide hormones should be technically straightforward.

METHODS

Methods and any associated references are available in the [online version of the paper](#).

Note: Any Supplementary Information and Source Data files are available in the [online version of the paper](#).

ACKNOWLEDGMENTS

This research was supported by the US National Institutes of Health (GM056414 (to S.H.G.) and NIDDK-11794 (to T.J.G.)). R.W.C. was supported in part by a National Institutes of Health Biotechnology Training grant (T32 GM008349).

AUTHOR CONTRIBUTIONS

R.W.C. and S.H.G. developed the underlying molecular designs, all authors participated in the design and execution of experiments to assess new compounds, and all contributed to data interpretation. S.H.G. and R.W.C. wrote the paper with input from all other authors.

COMPETING FINANCIAL INTERESTS

The authors declare competing financial interests: details are available in the [online version of the paper](#).

Reprints and permissions information is available online at <http://www.nature.com/reprints/index.html>.

1. Vilardaga, J.P., Romero, G., Friedman, P.A. & Gardella, T.J. *Cell. Mol. Life Sci.* **68**, 1–13 (2011).
2. Serada, M. *et al. Xenobiotica* **42**, 398–407 (2012).
3. Uzawa, T., Hori, M., Ejiri, S. & Ozawa, H. *Bone* **16**, 477–484 (1995).
4. Horne, W.S. *et al. Proc. Natl. Acad. Sci. USA* **106**, 14751–14756 (2009).
5. Johnson, L.M. & Gellman, S.H. *Methods Enzymol.* **523**, 407–429 (2013).
6. Wade, D. *et al. Proc. Natl. Acad. Sci. USA* **87**, 4761–4765 (1990).
7. Chongsiriwatana, N.P. *et al. Proc. Natl. Acad. Sci. USA* **105**, 2794–2799 (2008).
8. Porter, E.A., Wang, X.F., Lee, H.S., Weisblum, B. & Gellman, S.H. *Nature* **404**, 565 (2000).
9. Schievano, E. *et al. Biopolymers* **70**, 534–547 (2003).
10. Peggion, E. *et al. Biochemistry* **41**, 8162–8175 (2002).
11. Underwood, C.R. *et al. J. Biol. Chem.* **285**, 723–730 (2010).
12. Denton, E.V. *et al. Org. Lett.* **15**, 5318–5321 (2013).
13. Boersma, M.D. *et al. J. Am. Chem. Soc.* **134**, 315–323 (2012).
14. Pioszak, A.A. & Xu, H.E. *Proc. Natl. Acad. Sci. USA* **105**, 5034–5039 (2008).
15. Hoare, S.R.J., Gardella, T.J. & Usdin, T.B. *J. Biol. Chem.* **276**, 7741–7753 (2001).
16. Okazaki, M. *et al. Proc. Natl. Acad. Sci. USA* **105**, 16525–16530 (2008).
17. Feinstein, T.N. *et al. Nat. Chem. Biol.* **7**, 278–284 (2011).
18. Binkowski, B.F. *et al. ACS Chem. Biol.* **6**, 1193–1197 (2011).
19. Winer, K.K., Sinaii, N., Peterson, D., Sainz, B. & Cutler, G.B. *J. Clin. Endocrinol. Metab.* **93**, 3389–3395 (2008).
20. Kostenuik, P.J. *et al. J. Bone Miner. Res.* **22**, 1534–1547 (2007).

ONLINE METHODS

Binding and cAMP assays. Reported IC_{50} and EC_{50} values are the average of ≥ 4 independent assays (**Supplementary Tables 1–4**). Binding and cAMP assays were run in sample sizes comparable to those used in past work¹⁶, which provided data adequate for identifying differences in binding affinities and cAMP-inducing potencies. Each assay consists of ≥ 7 data points (different concentrations) per α/β -peptide, with each data point representing the average from duplicate wells. Binding to the RG and R^0 conformations of human or rat PTHR1 was assessed by competition assays performed in 96-well plates by using membranes from transiently transfected COS-7 cells as previously described¹⁶. In brief, binding to R^0 was assessed by using ^{125}I -PTH(1–34) as tracer radioligand and including GTP γ S in the reaction mixture (1×10^{-5} M). Binding to RG was assessed by using membranes containing a high-affinity, negative-dominant $G_{\alpha S}$ subunit ($G_{\alpha S}$ ND), and ^{125}I -M-PTH(1–15) as tracer radioligand. Previous work demonstrates that RG binding shows better correlation with cAMP potency than R^0 binding¹⁶. This finding is consistent with data presented in **Supplementary Fig. 2**. Alternatively, R^0 binding shows better correlation with the duration of calcemic responses induced *in vivo*¹⁶. This finding is consistent with the more transient nature of the calcemic response induced by **B5** compared to PTH(1–34), although the slight diminution in agonist potency of **B5** relative to PTH(1–34) implied by the rPTH1 data (**Supplementary Table 4**) may also contribute to the weaker *in vivo* response induced by **B5** relative to PTH(1–34).

cAMP signaling was assessed using HEK-293-derived cell lines that stably express the Glosensor cAMP reporter (Promega Corp.)¹⁸ along with either the wild-type human PTHR1 (GP-2.3 cells) or wild-type rat PTHR1 (GR-35 cells). These cells were tested for mycoplasma contamination. For cAMP dose–response assays, monolayers of confluent HEK 293 cells were pre-incubated with buffer containing d-luciferin (0.5 mM) in 96-well plates at room temperature until a stable baseline level of luminescence was established (30 min). Varying concentrations of agonist were then added, and the time course of luminescence response was recorded using a PerkinElmer plate reader following peptide addition. The maximal luminescence response (observed 12–16 min after ligand addition) was used for generating dose–response curves. (See **Supplementary Tables 1–4** and **Supplementary Figs. 3** and **4** for complete descriptions of binding and cAMP-induction assay results (including EC_{50}/IC_{50} values, s.e.m., E_{max} and p values) and composite binding and cAMP response curves.) These analyses assume Gaussian distribution of data, which is supported by the distribution of EC_{50} values for PTH(1–34)- and α/β -peptide-induced cAMP production in hPTH1-expressing cells presented in **Supplementary Data File 1**.

In vivo pharmacology: calcemic response. Mice (C57BL/6, male, age 9–12 weeks) were treated in accordance with the ethical guidelines adopted by Massachusetts General Hospital. Calcemic response assays were run in sample sizes comparable to those used in past work¹⁶, which provided data adequate for identifying differences in the time course and magnitude of PTH-induced calcemic responses. Statistical analyses were carried out assuming Gaussian distribution of data as supported by the distribution of blood ionized calcium levels presented in **Supplementary Data File 2**. Mice ($n = 5$ per compound) were injected subcutaneously with vehicle (10 mM citric acid/150 mM NaCl/0.05% Tween-80, pH 5.0) or vehicle containing PTH(1–34) or α/β -peptide at a dose of 20 nmol/kg body weight. Prior to injection, mice were grouped according to basal blood calcium concentrations to ensure each group possessed similar average (mean) blood ionized calcium levels at $t = 0$. A predetermined number of mice possessing the highest and lowest basal blood calcium concentrations were excluded from these studies. Groups were not statistically different on the basis of mean basal blood calcium concentration or body weight. Blood was withdrawn just before injection ($t = 0$) or at times thereafter. Tail vein blood was collected and immediately used for analysis. Blood Ca^{2+} concentration was measured with a Chiron Diagnostics model 634 Ca^{2+} /pH analyzer.

In vivo pharmacology: pharmacokinetics. Pharmacokinetic assays were run in sample sizes comparable to those used in past work¹⁶, which provided data adequate for identifying differences in PTH pharmacokinetic profiles using methodology described here. Statistical analyses were carried out

assuming Gaussian distribution of data as supported by the distribution of raw luminescence responses induced by plasma administration presented in **Supplementary Data File 3**. Blood content of PTH(1–34) or α/β -peptide analog was assessed in plasma from mice ($n = 3$) injected with vehicle or vehicle containing PTH(1–34) or an α/β -peptide at a dose of 20 nmol/kg body weight in an experiment performed separately from the calcemic response assays described above. Blood was withdrawn just before injection ($t = 0$) or at times thereafter. Tail vein blood was collected and treated with protease inhibitors (aprotinin, leupeptin, EDTA), centrifuged to remove blood cells, mixed with cAMP response assay buffer and administered to GP2.3 cells (see binding and cAMP assays section of online methods). The raw luminescence readouts recorded in this assay were converted to blood peptide concentrations through use of a standard curve relating luminescence response to known peptide concentrations under identical assay conditions (**Supplementary Fig. 5**). Previous work has demonstrated that this cAMP response–based method for quantifying the blood concentrations of PTHR1 agonists yields results similar to those from an enzyme-linked immunosorbent assay–based method¹⁶. GP2.3 cells exposed to plasma from mice injected with vehicle showed negligible luminescence responses, indicating that observed cAMP responses were dependent on the presence of a PTHR1 agonist.

Protease susceptibility assays. A high-performance liquid chromatography (HPLC) assay was used to assess proteolytic susceptibility⁴. Peptide concentration was determined by UV-vis spectroscopy (calculated from the UV-vis absorption at 280 nm, $\epsilon_{280nm} = 5,690 \text{ M}^{-1}\text{cm}^{-1}$ for all peptides except D6 and D7, for which $\epsilon_{280nm} = 11,380 \text{ M}^{-1}\text{cm}^{-1}$ was used; these values are based on an extinction coefficient for the tryptophan side-chain chromophore of $5,690 \text{ M}^{-1}\text{cm}^{-1}$). Peptide stock solutions were prepared in degassed water to a concentration of 200 μM . Sequencing-grade trypsin from bovine pancreas was purchased from Sigma-Aldrich and prepared to a stock concentration of 100 $\mu\text{g}/\text{ml}$ in 1 mM HCl. The protease reaction was carried out in 0.6 ml Eppendorf tubes at room temperature. The reaction solution was prepared by combining 40 μl of 200 μM peptide (final concentration 40 μM), 20 μl of $10\times$ TBS pH 8.5 (final concentration 15 mM Tris, 150 mM NaCl or $1\times$ TBS), 130 μl of water and 10 μl of 100 $\mu\text{g}/\text{ml}$ protease (added last, final concentration 5 $\mu\text{g}/\text{ml}$, in a total volume of 200 μl). Each proteolysis experiment was run in duplicate. Following addition of protease, the reaction was timed and quenched by combining a 50 μl aliquot of the proteolysis mixture with 50 μl of 0.1% trifluoroacetic acid in acetonitrile. A portion (75 μl) of the quenched reaction mixture was injected onto an analytical RP-HPLC (see **Supplementary Note 1** for description of HPLC conditions), and peaks were analyzed. The time course of peptide degradation was experimentally determined by integrating the area of the peak corresponding to the non-hydrolyzed peptide in a series of HPLC traces, with duplicate proteolysis reactions being used to generate error bars corresponding to the s.d. The final 50 μl of the reaction solution was used to acquire matrix-assisted laser desorption/ionization–time of flight (MALDI-TOF) mass spectrometry data for identification of peptide fragments resulting from proteolysis. Proteolysis was observed at all predicted trypsin cut sites for PTH(1–34). Shown in **Supplementary Figure 1** are time course data for peptide degradation (exponential decay curves and half-life values were generated using GraphPad Prism) and the trypsin cleavage sites in each substrate (based on MALDI-TOF-MS data).

Peptide synthesis. See **Supplementary Note 2** for synthetic methodology; **Supplementary Figure 6** for sequences and **Supplementary Figure 7** for analytical HPLC retention times, purity data and a list of observed masses from MALDI-TOF-MS (monoisotopic $[M+H]^+$, m/z); **Supplementary Figure 8** for HPLC traces and MALDI-TOF mass spectra.

Data calculations. Data were processed by using the Microsoft Excel and GraphPad Prism 4.0 software packages. Data from binding and cAMP dose–response assays were analyzed using a sigmoidal dose–response model with variable slope as previously used for analysis of data of this type¹⁶. Data sets were statistically compared by using Student's t test (two-tailed) assuming unequal variances for the two sets. Statistical calculations were carried out assuming Gaussian data distribution. This assumption is supported by data provided in **Supplementary Data Files 1–3**.